IJE TRANSACTIONS A: Basics Vol. 30, No. 10, (October 2017) 1583-1591

International Journal of Engineering

Journal Homepage: www.ije.ir

Effect of Blade Design Parameters on Air Flow through an Axial Fan

N. Rajabi, R. Rafee*, S. Frazam-Alipour

Faculty of Mechanical Engineering, Semnan University, Semnan, Iran

PAPER INFO

Paper history:
Received 18 April 2017
Received in revised form 03 July 2017
Accepted 07 July 2017

Keywords:
Axial Fan
Numerical Simulation
Turbulent Flow
Fan Blade Design
Number of Blades

ABSTRACT

The objective of this paper is the numerical study of the flow through an axial fan and examining the effects of blade design parameters on the performance of the fan. The axial fan is extensively used for cooling of the electronic devices and servers. Simulation of the three-dimensional incompressible turbulent flow was conducted by numerical solution of the (RANS) equations for a model. The *SST*- k-ω and k-ε turbulence models are applied in the simulations which are done using *CFX* software. The comparison between available experimental data and simulation results indicates that the *SST* k-ω model gives more accurate results than the k-ε model. The results also show that in separation regions and vortices, the pressure will decrease. Hub area and blade root contain large vortices. The effects of changes in the blade geometry and the number of blades on the fan performance are studied in detail. For the primary fan model with the different number of blades (4, 5, and 6), the maximum mass flow rate of 800 CFM is obtained. Hence, the number of blades had negligible effects on the maximum flow rate. By 3o% decreasing in the chord of the blades, the maximum mass flow rate of the fan with the different number of blades (5, 6 and 8) will be reduced to 500 CFM. Therefore, in order to increase the maximum mass flow rate, the chord and the width of blades should be increased. On the other hand, by increasing blades from 4 to 6 in the primary model, the maximum outlet pressure has been increased by 32%. Furthermore, it was found that in high flow rates, an increment in the number of blades had no effect on the produced static pressure.

***doi**: 10.5829/ije.2017.30.10a.20*

NOMENCLATURE

ρ	Fluid density (kg/m^3)	Γ_ω	Effective diffusivity of ω ($\frac{kg}{ms}$)
μ	Dynamic viscosity (kg/ms)	S_k & Y_k	User-defined source terms (kg/ms^3)
$\vec{\Omega}$	Rotational velocity (rad/s)	η	Fan efficiency (-)
$\tilde{G}_k$	Generation of turbulence kinetic energy (kg/ms^3)	ΔP	Pressure difference (Pa)
G_ω	Generation of ω (kg/m^{3}s^2)	Q	Air volume delivered by the fan (m^3/s)
Γ_k	Effective diffusivity of k ($\frac{kg}{ms}$)	p_i	Power used by the fan (Watt)

1. INTRODUCTION

In this paper, the turbulent flow in a subsonic axial fan is studied. Nowadays, studying the turbomachinery problems are feasible with the help of numerical methods. This study is a novel approach to evaluate the effects of different parameters on the performance of a fan by numerical simulations. Some important phenomena, which affect the fan operation should be considered before the manufacturing process.

*Corresponding Author's Email: Rafee@semnan.ac.ir (R. Rafee)

Ayremlouzadeh and Ghafouri [1] designed high flow rate vertically suspended pumps (VSPs) by employing CFTurbo application. They implemented the ANSYS-FLUENT Software to obtain the hydraulic profiles of diffuser blades. They employed SIMPLE algorithm and k-ε turbulence model to analyze the pressure distribution in different flow ranges. Finally, the comparison of the CFD simulations and experimental results indicated that they are in good agreement even at high flow rates.

Vazifeshenas et al. [2] studied the cavitation phenomenon of a four blade mixed flow pump which is

Please cite this article as: N. Rajabi, R. Rafee, S. Frazam-Alipour, Effect of Blade Design Parameters on the Air Flow through an Axial Fan, International Journal of Engineering (IJE), TRANSACTIONS A: Basics Vol. 30, No. 10, (October 2017) 1583-1591

influenced by flow rate, rotational speed and saturation pressure of the fluid in a particular temperature. They employed RNG k-ε turbulence model and standard wall function for near wall treatment. They determined the cavitation regions in different cases and figured out that the temperature variations caused by weather changes have not significant effect on the cavitation.

Amanifard [3] studied the rotating-stall-like phenomena in an axial compressor by employing the VAN Leer's Flux splitting algorithm and TVD limiters in the numerical simulations. Also, the turbulence model of Baldwin-Lomax has been used. The oscillatory velocity traces indicated a periodic trend of vortices which caused a decrease in the mass flow rate.

Ghorbanian et al. [4] studied the vortices and flow properties of an axial compressor during the instability condition. They developed an unsteady two-dimensional finite volume solver by applying Van Leer's algorithm and employed Baldwin-Lomax (BL) turbulence model. They figured out that the decrement in mass flow rate, the positive pressure gradient and multi-blade cascade are the factors which affect the generation of vortices in this case.

Krishna and Ramji [5] performed a numerical simulation of the noise production of cooling fans. Also, they substituted the NACA 65-010 with their current blade to reach the lowest noise production with the magnitude of 65.4 (dB).

Hu et al. [6] studied the effect of the casing on the generated noise of the axial fan. They realized that the scattering effect of the duct should be included in the prediction of the noise.

Scheit et al. [7] studied the effect of the pitch angle of the radial fan's blade on its noise production. To this purpose, they utilized experimental and numerical methods. The results indicated no vibration declining by increasing aerodynamic efficiency. Hurault et al. [8] studied the effect of sweep angle of blades. Their experimental and numerical investigations were performed for three blades with different types of sweep angles (forward, backward and no sweep angle). They realized that the forward sweep angle would change the radial component of velocity and the backward sweep angle will increase this component. Lin and Huang [9] applied experimental and numerical methods for a centrifugal fan equipped with forwarding sweep angle blade with the casing. In order to design the blades, the NACA 4412 profile had been chosen. Then, a real scale model of their fan was made by CNC. After validating the numerical simulations with experimental data, they found CFD methods as a reliable tool to design turbomachines. Pathak et al. [10] studied the flow in a single stage blower by the k-ε turbulence model. They found that the outlet pressure coefficient would be plummeted dramatically by the increasing the flow rate. Denton [11] performed a research on the errors of the numerical simulation of the turbomachines and their restrictions. For instance, fluid-domain restrictions, modeling deficiency, turbulent modeling errors, complicated boundary conditions and elaborate geometry (clearances and blades edge shape) are the types of errors which were mentioned. Foss et al. [12] performed an experimental and numerical investigation to study the fan's reliability. Therefore, data which obtained by Hotwire device were categorized into velocity component and root means square fluctuation (RMSF) and compared with 3d simulations.

Chen et al. [13] studied the operation of fans by numerical simulations and experimental methods. The results which obtained from different types of velocities indicate that the numerical results were matched with experimental data. Furthermore, they studied the effects of axial clearance of fans, fans cover, and brackets.

Beiler and Carolus [14] studied the fans equipped with skewed cord blades by numerical simulations based on the frozen rotor assumption. Circumstances of cord skewness have been checked to make a comparison between the numerical and experimental methods. They realized that the designed fan was matched with the main fan from the aerodynamic point of view and noise production. Estevadeordal et al. [15] studied a low-speed axial fan by the digital particle image velocimetry (DPIV). They coordinated the bypass of blades by the cameras and lasers in order to measure the averaged time velocity on the leading edge, trailing edge, suction section and pressure magnitude on blade sides, then output results were compared with data of the panel codes. They realized that the local viscosity effects like separation region and flow fluctuation were not included in the panel method.

Zhang et al. [16] simulated the three-dimensional transient flow of an axial flow pump using the k-ε turbulence model. Results indicated that the accuracy of simulation in a transient simulation is 4.54 percent more than the steady state. Shigemitsu et al. [17] studied the operation of a small contra-rotating rotor fan. First, they indicated the significance of using contra-rotating rotors in small fans to improve the efficiency. Furthermore, they focused on the numerical simulation method of internal flow and its pressure distribution in order to describe the effects of contra-rotating rotors in fan operation. Lee et al. [18] studied the optimization of axial fans in low velocities by the three-dimensional solution of the RANS Equations in order to improve fan efficiency by modifying the blade profile, thickness, and their base support. They utilized a sort of gradient algorithms to optimize fan efficiency, so they conclude that modification of fan support is more effective compared to the changes in the blade profile. Venter and Kroger [19] studied the effect of the clearance between the casing and tip of the blades. They came up with the idea that the effect of the tip clearance on the

performance is related to the type of rotor, its size and methods of the installation. Vad and Bencze [20] performed a research on radial velocity components of three-dimensional flow in axial flow fans by Laser Doppler and proposed a linear formula in order to estimate averaged radial velocity at the outlet section. Li et al. [21] investigated the flow control with casing treatment in axial compressors by CFD solutions to increase flow range. They designed a counter-swirl self-recirculation casing for an axial fan rotor. They considered three different slot locations and realized that the largest flow range could be achieved by adjusting the slot at the most downstream area by using a 50% length of the baffle.

Axial flow fans have been used extensively in order to cool server's equipment or computer chips like CPUs. For instance, Central Processing Units (CPU) of the computers, depending on their process type would reach to critical thermal zones. In other words, a routine type of applications, like surfing the net requires lower process so the CPU power is in the minimum state, on the other hand, some applications like engineering software's would lead a processor into heavy tasks. Normally temperature zone for medium tasks is between 50 and 75 Centigrade so the cooling procedure which is used for these chipsets should be able to create a suitable thermal zone to guarantee their life cycle. In this research, different parameters required to design a fan was studied by numerical simulations. To validate this study, a significant comparison between numerical methods and experimental data has been done in order to determine the best turbulence model for the solution. Therefore, the reliability factor and accuracy of simulations has been investigated in the case of k-ε and SST k-ω turbulence models. Meanwhile, The most important factor which separates this paper from the others is the complete CFD study on the effects of the number of blades and their geometry on the produced outlet pressure and mass flow rate of the fan. In addition, the flow field and separation zones have been studied to describe the variations of pressure through the blades which are not previously done by the researchers.

2. GOVERNING EQUATIONS

Continuity equation:
The continuity equation for the relative velocity in the rotating frame is as below:

$$\frac{\partial \rho}{\partial t} + \vec{\nabla} \cdot (\rho \overrightarrow{V_r}) = 0 \quad (1)$$

In which $\overrightarrow{V_r}$ is the average velocity of fluid respect to the rotating frame in incompressible flow.
Navier-Stocks equations:
In stationary frame coordination with the rotational velocity of $\vec{\Omega}$, the Navier-Stocks equation for the average velocity is as following:

$$\frac{\partial \rho \overrightarrow{V_r}}{\partial t} + \vec{\nabla} \cdot (\rho \overrightarrow{V_r} \overrightarrow{V_r}) + \rho(2\vec{\Omega} \times \overrightarrow{V_r} + \vec{\Omega} \times \vec{\Omega} \times \overrightarrow{r}) = -\frac{\partial \bar{p}}{\partial x_i} + \vec{\nabla} \cdot (\bar{\bar{\tau}}_r) \quad (2)$$

In which:

$$\bar{\bar{\tau}}_r = (\mu + \mu_t)\left(\vec{\nabla}\overrightarrow{V_r} + \vec{\nabla}\overrightarrow{V_r}^T\right) - \frac{2}{3}\rho k \delta_{ij} \quad (3)$$

$SST\ k-\omega$ Model Transport Equations:
In order to calculate the turbulent viscosity of (μ_t) , the SST- k-ω model has been used. The transport equations are given by:

$$\frac{\partial}{\partial t}(\rho k) + \frac{\partial}{\partial x_i}(\rho k u_i) = \frac{\partial}{\partial x_j}\left(\Gamma_k \frac{\partial k}{\partial x_j}\right) + \tilde{G}_k - Y_k + S_k \quad (4)$$

$$\rho\omega\left(\frac{\partial}{\partial t} + \frac{\partial u_i}{\partial x_i}\right) = \frac{\partial}{\partial x_j}\left(\Gamma_\omega \frac{\partial \omega}{\partial x_j}\right) + G_\omega - Y_\omega + D_\omega + S_\omega \quad (5)$$

Also, the automatic wall function has been used with SST- k-ω model [22].
Axial fan efficiency is defined by

$$\eta = \frac{(\Delta P \times Q)}{p_i} \quad (6)$$

3. PROBLEM DEFINITION

Air flows at 25 °C with the density of ρ=1.18 kg/m^3 and the dynamic viscosity of μ=1.86×10^{-5} (kg/ms). The rotational speed is 2900 rpm.

To check the Validity of the simulations, a three-dimensional model of an industrial fan with 3 blades according to its drawings had been prepared by Solid Works software. Figure 1 demonstrates the dimensions of the hub and a blade. After the mesh generation and numerical simulation, the output data had been compared with the manufacturer characteristics curve. In addition, separation zones have been studied to describe pressure distribution and flow on blade sides. In order to simulate the fan flow in the CFX software, it's necessary to specify the flow domain of one blade with passages and set the number of blades, and then CFX would make a complete model of the fan using the periodic boundary conditions. According to Figure 2, the one-third of the fan was prepared in Solid Works.

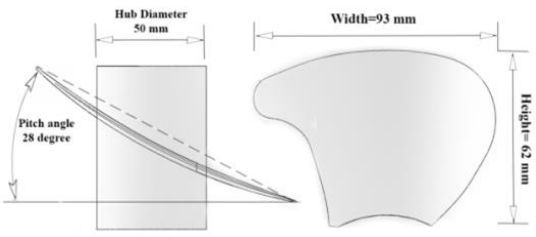

Figure 1. Geometry of the modeled fanof modeled Fan

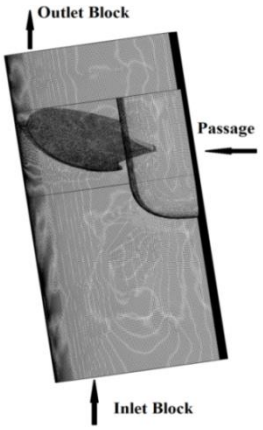

Figure 2. Meshes and Blocks.

Two stationary blocks are considered as the inlet block and the outlet block of flow domain then a passage block which includes the blade had been determined in the middle of two fixed blocks. ICEM- CFD was used to mesh the domain. The procedure of mesh generation was based on HEX dominant method since it is capable of raising the cell's density near the walls by inflation method and reduce cells density in non-sensitive domains which are far from walls by tetrahedral elements. In the computational fluid dynamics, especially in turbomachinery, Hexahedral Meshing will improve the accuracy of the simulation.

Turbo mode in CFX software is provided to simulate the flows in turbomachinery applications. It's possible to select the turbomachine type for a specific application in which meshing blocks have been made.

After specifying fluid domains and boundary conditions, the passage block of the fan is considered to have the rotational speed of 2900 rpm. Two turbulence models of SST- k-ω and k-ε had been used to check the accuracy of simulations.

4. NUMERICAL RESULTS

Seven simulations at 7 different flow rates for each of turbulence models had been performed in order to make a comparison with experimental data. In this paper, the characteristics curves which are released by the manufacturer[2], are used as the experimental data for validation of the simulation.

4. 1. Boundary Conditions It is assumed that the heat transfer is negligible. According to Table 1, the one-atmosphere pressure at the inlet section and mass flow rate at the outlet section are specified as the boundary conditions. The fluid is assumed to be incompressible, the outlet volumetric flow rate (in CFM) had been converted to mass flow rates. Then, the mass flow rate was specified at the outlet. For instance, at the flow rate of 400 CFM, the outlet mass flow rate of 0.222 (kg/s) is applied. At the inlet boundary, the total pressure is 1 atmosphere. Periodic boundary conditions are applied for all of the blocks to model the fan with defined number of blades. So, it doesn't need to model the full domain of the fan. On the walls, the no-slip wall condition was applied. For turbulent quantities, the automatic wall functions [22] was applied in the near wall cells. The simulations were conducted in steady state condition and the turbulence intensity of 5% is applied at the inlet. The maximum residual of 10^{-5} is applied for termination of the numerical iterative solution of each equation.

As shown in Figure 3, It's concluded that the numerical results obtained by SST- k-ω model are more accurate than those obtained by k-ε model.

The greatest error of the results of SST- k-ω turbulence model at the flow rate of 500 (CFM) is 15%. While the maximum error in the simulations with the k-ε model is 50 %. Therefore, the SST- k-ω model is more accurate than the k-ε model to simulate the problem. Therefore, others simulations of this study were based on SST- k-ω turbulent model.

TABLE 1. Boundary conditions for 7 simulations in different flow rates

Volumetric flow rate (CFM)	Boundary type	
	Total inlet Pressure (atm)	outlet mass flow rate (kg/s)
200	1	0.111
300	1	0.167
400	1	0.222
500	1	0.278
600	1	0.334
700	1	0.389
800	1	0.445

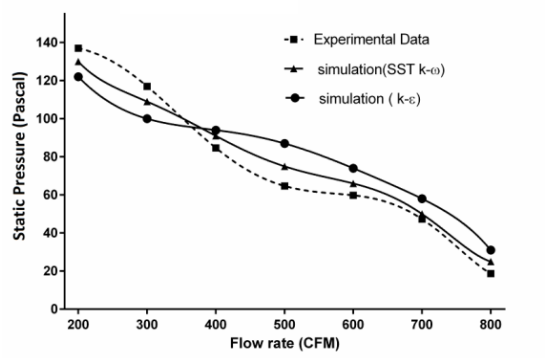

Figure 3. Comparison between simulation results and manufacturer's experimental data

[2] http://www.sunon.com/

4. 2. Grid Independence Test In order to reach the best cells arrangement, grid independence was studied in the volumetric flow rate of 400 CFM for different grids. The dimensionless distance from the first cell adjacent to the wall (y^+) is less than 5 in SST-k-ω turbulent models and the automatic wall functions are used for near wall cells.

The outlet static pressure and a related number of elements have been shown for three different types of meshing in Table 2. According to the table, the outlet pressure of the simulations with 3420651 and 2988237 elements have produced the same static pressure at outlet section. Thus, the results of the simulations with 2988237 elements are grid independent.

4. 3. Pressure Distribution and Flow Separation Study Figure 4 shows velocity vectors on the outlet section of the fan. As can be seen, due to vortex generation at the center of fan the velocity of flow in the areas far from the center is dramatically higher than that in the central zone. For models with smaller hubs, the generated vortex is smaller.

Pressure distribution at the flow rate of 400 CFM along a streamline from the inlet of the fan to its outlet has been shown in Figure 5. As shown, the total pressure is almost constant at the inlet block. However, when the fluid particles reach the inlet of the rotor block, the flow area decreases because there is a fan hub. Area reduction causes the increment in the velocity and reduces the static pressure. There are also separation zones on the rear side of the blades at leading edge.

The blades give the energy to the flow and the static pressure will rise. When the fluid particles reach the outlet block, the flow area decreases because there is a separation zone in this region. Therefore, at the start of the outlet block, the velocity increases which leads to a reduction in the static pressure.

TABLE 2. SST_ k-ω model grid independence test results

Number of cells	3420651	2988237	1735268
Outlet static pressure (Pascal)	91	91	73

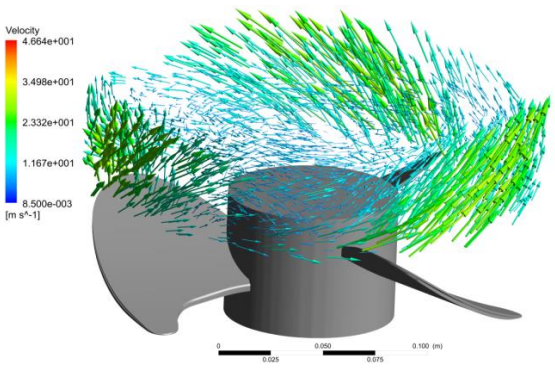

Figure 4. Velocity vectors on the fan exit

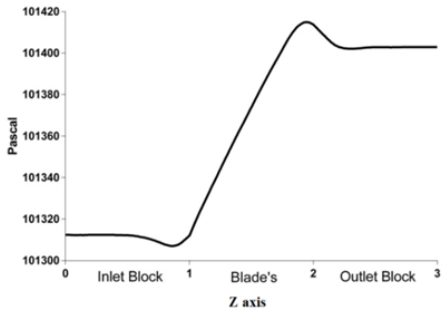

Figure 5. Pressure distribution on z-axis at 400 CFM

Before the fluid enters the rotational block (blades), the pressure reaches to its lowest value in the streamline passes the root of the blades. In this region, the fluid particles accelerate and pressure reduces (It is almost 10 Pascals lower than the inlet pressure).

As mentioned before, the pressure declined just at the beginning of the rotational block. Figure 6 shows the pressure contours on the rear side of a blade at the flow rate of 400 CFM. When the air flows on the leading edge of the blade, the separations occurs and the pressure decreases. Near the trailing edge, there is no separation, and the pressure is higher in this region. So, the pressure will increase from leading edge to trailing edge. To realize the pressure drop at the beginning of rotating block, the separation zone and velocity vectors are studied in 4 different cross-sections of a blade (Figure 7).

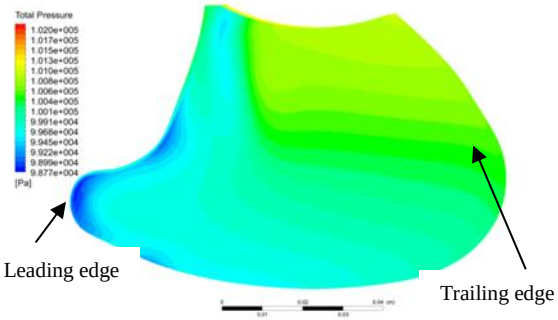

Figure 6. Contours of the pressure on the rear side of a blade at the flow rate of 400 CFM

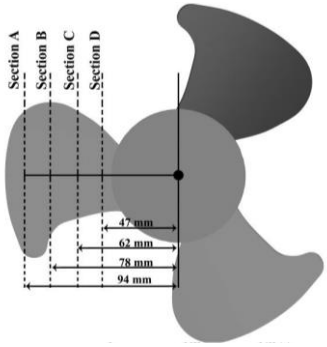

Figure 7. locations of the sections on a blade

Also Figure 8 indicates the velocity vectors related to sections A, B, C and D and demonstrates the flow separation zones over the blade in different sections from tip to the root of the blade. Flow separations in the base of the blade are dramatically larger (section D) and it shows a downward trend by approaching to the blade tip (section A).

This phenomenon explains pressure drop on the rear side of the blade. Vortices which are generated by a blade in a rotational motion causes a decrease in the fan efficiency because of the direction change of the main flow and cause the hydraulic losses.

In order to increase fan efficiency, vortices generation and separation zones should be reduced with practical methods. For instance, the pitch angle of the blade could be optimized to reduce separation and better blade profiles could be selected.

On the other hand, by reducing the rotational speed of the fan, the flow separations decreases. For a fan with 3 blades, the effects of rotational speed have been investigated numerically. Results indicate that for the speed of 2600 rpm (at the flow rate of 400CFM), the separation zones and vortices are smaller than those for 2900 rpm. The pressure differences in rotational speeds of 2900 and 2600 rpm are 90 and 76 Pascal, respectively. Regarding experimental characteristic curve of this fan[3], the power consumption for the rotational speed of 2900 and 2600 rpm is 120 and 88 Watts, respectively. According to Equation 6, the efficiency of this 3-blade fan with 400 CFM flow rate at 2600 and 2900 rpm is 19% and 16%, respectively. So, it can be concluded that by decreasing separations the fan efficiency is improved significantly.

4. 4. Effects of Design Parameters and Discussion

First, the effect of changes in rotational speed on the outlet pressure has been studied. Then, pressure and flow rate changes have been investigated for the fans with more number of blades. Finally, by modifying blade geometry and its quantity in different flow rates, the outlet pressure has been predicted and discussed.

4. 4. 1. Changes In Rotational Speed In this case, the outlet pressure of a 3-blade fan has been predicted at the flow rate of 400 (CFM) in different rotational speeds by numerical simulations. These changes have been specified in six different rotational speeds from 1900 to 4400 rpm. According to Figure 9, increasing the rotational speed provides a significant improvement in the produced static pressure.

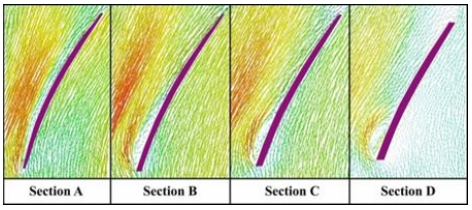

Figure 8. Velocity vectors on different sections and separation zones

[3] http://www.sunon.com/

4. 4. 2. Changes in the Number of Blades In this case, the rotational speed has been considered to be constant at 2900 rpm and changes have been made in a number of blades according to Figure 10.

Thus, three types of fans had been modeled which consists of 4, 5 and 6 blades, respectively.

The process of grid generation is similar to that of a 3-blade fan. For each model, numerical simulation has been conducted in seven different flow rates and their outlet pressures were predicted.

All of the boundary conditions are the same as mentioned in Table 1. Three different characteristic curves for fan models with the 4, 5 and 6 number of blades are obtained in this section (see Figure 11).

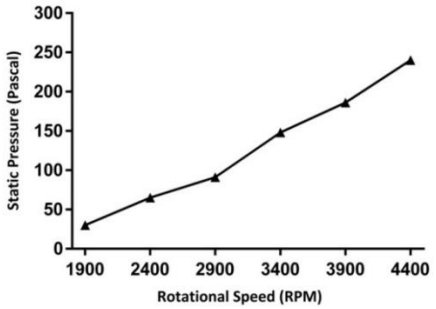

Figure 9. Pressure changes in different speed in constant flow rate

Figure 10. Changes in number of blades

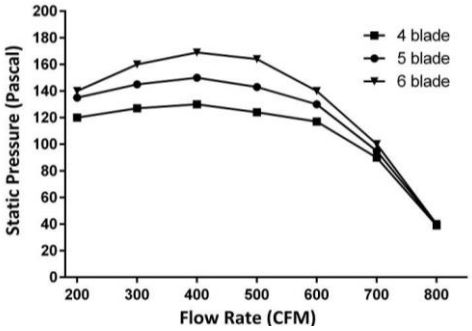

Figure 11. Characteristics curves of the fans with the different number of blades

Characteristic curves in Figure 11 indicate that by increasing the flow rate from 200 CFM to 400 CFM the pressure will increase. However, increasing the flow rate from 400 CFM to 800 CFM reduces the static pressure significantly. Applying more number of blades (from 4 to 6) causes about 32% increase in maximum pressure at 400 CFM. By applying more number of blades, the contact surface between the blades and fluid increases and more energy transfer occurs. Therefore, the outlet pressure increases. At high flow rates, the big separations occur and applying more number of blades can not increase the outlet pressure significantly. Figure 11 indicates that the produced static pressure for the different number of blades at the maximum flow rate of 800 (CFM) is almost equal to 42 Pascal. As a result, increasing the number of blades can not affect the range of flow rate. However, it will raise the outlet static pressure.

4. 4. 3. Changes in Geometry of Blades for the Secondary Model In this step, changes have been made to the geometry and number of blades. Firstly, a new blade was designed by the same profile, identical pitch angle and smaller width. Then, the number of blades has been increased in three steps. So three different types of a fan with smaller blades consist of 5, 6 and 8 blades had been modeled. Also, the process of meshing is the same as mentioned for the 3-blade fan. Figure 12 shows new models of the fan. The rotational speed is assumed to be constant (2900 rpm).

All of the assigned boundary conditions are defined in Table 1. Hence, the outlet gauge pressure obtained from numerical simulations for each of fans in three different types of blades and seven various flow rates. The predicted characteristics curves are shown in Figure 13 and it indicates a sharp trend of pressure decrement by increasing flow rate. By applying more number of blades, more energy is transferred to the airflow and higher outlet pressures are obtained. The comparison between Figure 11 and 13 indicates that the fans with more number of smaller blades will produce greater pressures in lower flow rates. For instance, in the flow rate of 200 CFM for primary models, the fan with 6 larger blades produced the outlet pressure of 140-Pascal while in the secondary models the fan with 6 smaller blades produced the outlet pressure of 200-Pascal.

Despite the Figure 11, All of the predicted curves have a downward trend in Figure 13.

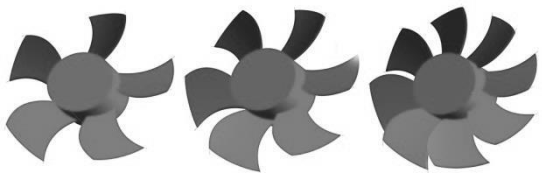

Figure 12. changes in the geometry and number of blades

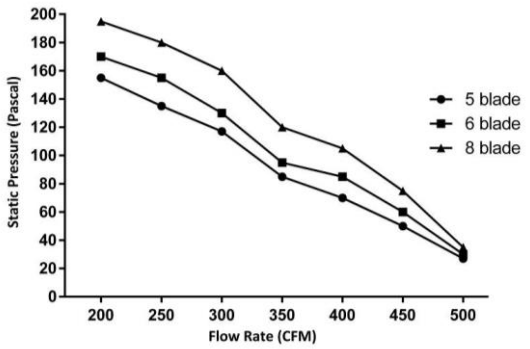

Figure 13. Characteristics curves of the fan for different geometries and number of blades.

Hence, it can be concluded that the trends of characteristic curves depend on the blade geometry.

It can be vividly seen that by increasing the number of blades, higher pressures will be obtained. For instance, the average pressure increment by adding one blade to a 5-blades fan is about 12% and the pressure increment by adding 3 blades to a 5-blades fan is about 26%.

By decreasing the blade width, lower air flow will be obtained so there would be a reduction in the flow rate. At the flow rate of 500 (CFM), the produced static pressure for each of fans is about 34 Pascal in secondary models. Therefore, it is concluded that the range of flow rate depends on the blade geometry. On the other hand, the range of the static pressure depends on the number of blades.

5. CONCLUSION

According to numerical simulations and comparison with the experimental data, *SST* k-ω turbulence model has more accurate results compared to the k-ε model. In addition inlet, pressure plummeted from the first block and reaches to its lowest at the beginning of the rotor block. The separation of the flow occurs at the rear side of the leading edge of blades and vertices cause the pressure drop. As bigger the separation zone is, the pressure loss is greater and the efficiency is lower. So, it's crucial to optimize the fan design since pitch angle and blade profile is effective items in order to improve efficiency. At lower rotational speeds, the flow separation regions are smaller and the efficiency is higher. For instance, the efficiencies of a 3 blade fan at speeds of 2600 and 2900 RPM are 19% and 16%, respectively.

Along the rotational block, the pressure increases and hits the highest at the end of this part. By increasing the rotational speed of the fan, the outlet pressure in constant flow rate increases linearly. Increasing the

number of blades for the primary model in constant rotational speeds and flow rates produces higher outlet pressure up to 32% at 400 CFM. In this case, all of the models have the same produced pressure (40 Pascal) at highest flow rate (800 CFM).

Finally, by miniaturizing blades size and increasing their quantity, higher outlet pressures up to 196 Pascal in lower flow rates will be obtained. The maximum flow rate of a fan is independent of the number of blades but it is directly related to blade size and geometry.

6. REFERENCES

1. Ayremlouzadeh, H. and Ghafouri, J., "Computational fluid dynamics simulation and experimental validation of hydraulic performance of a vertical suspended api pump (research note)", ***International Journal of Engineering-Transactions B: Applications***, Vol. 29, No. 11, (2016), 1612-1620.
2. Vazifeshenas, Y., Farhadi, M., Sedighi, K. and Shafaghat, R., "Numerical simulation of cavitation in mixed flow pump", ***International Journal of Engineering-Transactions C: Aspects***, Vol. 28, No. 6, (2015), 956-962.
3. Amanifard, N., "Stall vortex shedding over a compressor cascade (research note)", ***International Journal of Engineering-Transactions A: Basics***, Vol. 18, No. 1, (2004), 29-36.
4. Ghorbanian, K. and Amanifard, N., "A numerical investigation on the unstable flow in a single stage of an axial compressor", ***International Journal of Engineering-Transactions A: Basics***, Vol. 16, No. 2, (2003), 171-180.
5. Krishna, S.R., Krishna, A.R. and Ramji, K., "Reduction of motor fan noise using CFD and caa simulations", ***Applied acoustics***, Vol. 72, No. 12, (2011), 982-992.
6. Hu, B.-b., OuYang, H., Wu, Y.-d., Jin, G.-y., Qiang, X.-q. and Du, Z.-h., "Numerical prediction of the interaction noise radiated from an axial fan", ***Applied acoustics***, Vol. 74, No. 4, (2013), 544-552.
7. Scheit, C., Karic, B. and Becker, S., "Effect of blade wrap angle on efficiency and noise of small radial fan impellers—a computational and experimental study", ***Journal of Sound and Vibration***, Vol. 331, No. 5, (2012), 996-1010.
8. Hurault, J., Kouidri, S., Bakir, F. and Rey, R., "Experimental and numerical study of the sweep effect on three-dimensional flow downstream of axial flow fans", ***Flow Measurement and Instrumentation***, Vol. 21, No. 2, (2010), 155-165.
9. Lin, S.-C. and Huang, C.-L., "An integrated experimental and numerical study of forward–curved centrifugal fan", ***Experimental Thermal and Fluid Science***, Vol. 26, No. 5, (2002), 421-434.
10. Pathak, Y.R., Baloni, B.D. and Channiwala, D.S., "Numerical simulation of centrifugal blower using CFX", ***International Journal of Electronics, Communication & Soft Computing Science and Engineering***, (2012), 242-247.
11. Denton, J.D., "Some limitations of turbomachinery CFD", ***ASME Paper No. GT2010-22540***, (2010), 735-745.
12. Foss, J., Neal, D., Henner, M. and Moreau, S., "Evaluating CFD models of axial fans by comparisons with phase-averaged experimental data". (2001), SAE Technical Paper.
13. Chen, Y.-C., Chen, C.-L. and Dong, Q., "CFD modeling for motor fan system", in Electric Machines and Drives Conference. IEMDC'03. IEEE International, Vol. 2, (2003), 764-768.
14. Beiler, M. and Carolus, T., "Computation and measurement of the flow in axial flow fans with skewed blades", ***Transactions-American Society of Mechanical Engineers Journal of Turbomachinery***, Vol. 121, (1999), 59-66.
15. Estevadeordal, J., Gogineni, S., Copenhaver, W., Bloch, G. and Brendel, M., "Flow field in a low-speed axial fan: A dpiv investigation", ***Experimental Thermal and Fluid Science***, Vol. 23, No. 1, (2000), 11-21.
16. ZHANG, D.-s., SHI, W.-d., Bin, C. and GUAN, X.-f., "Unsteady flow analysis and experimental investigation of axial-flow pump", ***Journal of Hydrodynamics, Ser. B***, Vol. 22, No. 1, (2010), 35-43.
17. Shigemitsu, T., Fukutomi, J. and Okabe, Y., "Performance and flow condition of small-sized axial fan and adoption of contra-rotating rotors", ***Journal of Thermal Science***, Vol. 19, No. 1, (2010), 1-6.
18. Lee, K.-S., Kim, K.-Y. and Samad, A., "Design optimization of low-speed axial flow fan blade with three-dimensional rans analysis", ***Journal of Mechanical Science and Technology***, Vol. 22, No. 10, (2008), 1864-1869.
19. Venter, S. and Kröger, D., "The effect of tip clearance on the performance of an axial flow fan", ***Energy Conversion and Management***, Vol. 33, No. 2, (1992), 89-97.
20. Vad, J. and Bencze, F., "Three-dimensional flow in axial flow fans of non-free vortex design", ***International Journal of Heat and Fluid Flow***, Vol. 19, No. 6, (1998), 601-607.
21. Li, X., Spence, S., Chen, H., Chu, W. and Gibson, L., "Flow control by slot position and noise baffle in a self-recirculation casing treatment on an axial fan-rotor", ***International Journal of Rotating Machinery***, Vol. 2017, (2017), 143-151.
22. ANSYS Inc, ANSYS-CFX, Release 16, Documentation, Reference Guide, (2016).

Effect of Blade Design Parameters on Air Flow through an Axial Fan

N. Rajabi, R. Rafee, S. Frazam-Alipour

Faculty of Mechanical Engineering, Semnan University, Semnan, Iran

P A P E R I N F O

Paper history:
Received 18 April 2017
Received in revised form 03 July 2017
Accepted 07 July 2017

Keywords:
Axial Fan
Numerical Simulation
Turbulent Flow
Fan Blade Design
Number of Blades

چکیده

هدف از این تحقیق تحلیل جریان عبوری از فن فروصوت محوری و بررسی پارامترهای طراحی پره آن است. فن های محوری کاربرد گسترده‌ای جهت خنک سازی قطعات الکترونیکی و سرورها دارند. شبیه سازی جریان آشفته سه بعدی عبوری از فن با حل عددی معادلات متوسط زمانی ناویر استوکس برای یک فن صنعتی انجام شده است. شبیه سازی‌ها در نرم‌افزار CFX با مدل‌های انتقال تنش برشی ($SST\ k\text{-}\omega$) و مدل آشفتگی k-ε انجام شده است. از مقایسه داده‌های تجربی و نتایج حل عددی مشاهده می‌شود که نتایج مدل $SST\ k\text{-}\omega$ *در این شبیه سازی* دقیق‌تر است. مشاهده می شود در نواحی تشکیل گردابه‌ها فشار خروجی از فن کاهش پیدا می کند، نواحی هاب و پایه پره‌ها بیشترین گردابه‌ها را در بر دارند. همچنین تاثیر تغییر اندازه پره‌ها و تعداد آن‌ها بر عملکرد فن مورد مطالعه قرارگرفته است. نتایج نشان می‌دهد برای مدل اولیه با تعداد پره های ۴ ، ۵ و ۶ حداکثر دبی جریان عبوری از فن برابر ۸۰۰ فوت مکعب بر دقیقه می باشد، در نتیجه تعداد پره‌ها تاثیری بر ماکزیمم دبی فن ندارد. با کوچکتر کردن وتر پره به اندازه ۳۰ درصد مقداره اولیه در مدل ثانویه، حداکثر دبی خروجی از فن با تعداد پره های ۵ ، ۶ و۸ به ۵۰۰ فوت مکعب بر دقیقه کاهش می یابد، پس نتیجه می شود به منظور افزایش دبی جریان می بایست پره هایی بزرگتر با عرض و پهنای بیشتر طراحی کرد. از سوی دیگر افزایش تعداد پره منجر به افزایش فشار بیشینه خروجی می شود. در مدل اولیه با افزایش تعداد پره از ۴ به ۶ میزان فشار بیشینه خروجی به میزان ۳۲ درصد افزایش یافته است. همچنین مشخص شد که در دبی‌های بسیار زیاد افزایش تعداد پره تاثیری بر افزایش فشار خروجی ندارد.

***doi**: 10.5829/ije.2017.30.10a.20*